STUDY OF DYNAMIC ABSORPTIVITY AT 10.6 µm (CO2) AND 1.06 µm (Nd-YAG) WAVELENGTHS AS A FUNCTION OF TEMPERATURE — Source link

C. Sainte-Catherine, Michel Jeandin, D. Kechemair, J.-P. Ricaud ...+1 more authors

Institutions: Mines ParisTech, Centre national de la recherche scientifique

Related papers:

- Laser-assisted machining of Inconel 718 with an economic analysis

- In situ absorptivity measurements of metallic powders during laser powder-bed fusion additive manufacturing

- Melting characteristics of metals by combined laser beams with different wavelength

- Modifications of AISI 1045 steel by picosecond Nd:YAG laser at 266 nm; comparison with 532 and 1064 nm pulses

- Surface modifications of AISI 1045 steel created by high intensity 1064 and 532 nm picosecond Nd:YAG laser pulses

Share this paper:

STUDY OF DYNAMIC ABSORPTIVITY AT 10.6 μm (CO2) AND 1.06 μm (Nd-YAG) WAVELENGTHS AS A FUNCTION OF TEMPERATURE

C. Sainte-Catherine, Michel Jeandin, D. Kechemair, J.-P. Ricaud, L. Sabatier

STUDY OF DYNAMIC ABSORPTIVITY AT 10.6 μm (CO_2) AND 1.06 μm (Nd-YAG) WAVELENGTHS AS A FUNCTION OF TEMPERATURE

C. SAINTE-CATHERINE[(1),*], M. JEANDIN*, D. KECHEMAIR**, J.-P. RICAUD** and L. SABATIER**

*Ecole des Mines de Paris, Centre des Matériaux P.M. Fourt, BP. 87, F-91003 Evry cedex, France
**Laboratoire d'Application des Lasers de Puissance, Unité Mixte ETCA/CNRS, 16 bis av. Prieur de la Côte d'Or, F-94114 Arcueil cedex, France

Abstract

One of the main advantages of Nd-YAG lasers compared to CO_2 lasers consists of easy beam handling using optical silica fibers. However, up to now Nd-YAG applications for material processing were limited due to a rather low available mean output power (less than about 500 W). A Eureka project (termed "EU-226") which consequently aimed at developing the so called "High Power Solid State Laser (HPSSL)" capable of 1 to 3 kW, involved absorptivity studies results of which are given in this contribution. Metallic surfaces exhibit a higher absorptivity at 1.06 μm (Nd-YAG) than at 10.6 μm which improves the energy transfer with a Nd-YAG laser and decreases the thermal runaway. This was acertained by measurements of absorptivity as a function of temperature and by thermal cycle calculations. This permits laser surface hardening of steels without any coating or gas shielding, which prevents in particular pollution. Various materials, i. e. pure nickel, Inconel 718 and AISI 1045 steel, were studied, featuring in particular the influence of surface roughness, oxidation and initial absorptivity on laser-material interaction.

Keywords

Laser, CO_2, Nd-YAG, Absorptivity, Surface Treatment, Thermal runaway, Steel, Nickel, Inconel 718, Eurêka.

Introduction

In laser surface treatments, the beam absorption can vary considerably depending on surface quality, temperature and environment. It is well known that metal surfaces show a great absorptivity increase when irradiated with a focused laser light. However, the exact mechanisms involved are not clear yet [1]. These would however be of a great interest to characterize the potential of new Nd-YAG lasers in high power systems capable of 1 to 3 kW and called "High Power Solid State Laser (HPSSL)" studied in Eureka project EU-226. Reliable data on absorption are therefore missing to accurately modelize the heat flow and field of temperature during for example laser hardening.

Two different methods for measuring the absorptivity respectively at 10.6 μm (CO_2) and 1.06 μm (Nd-YAG) were used. The first one, already used at I.S.L. (Institut Saint-Louis) [2] and E.T.C.A. [3], is based on temperature measurements ; the second one, for 1.06 μm, is optical using an integrating sphere [4].

Although laser processing is generally carried out with gas shielding, this preliminar study does not involve any gas protection and all measurements are done in air environment because careful control of the surrounding atmosphere is very difficult when using a mere nozzle.

[(1)] C. SAINTE-CATHERINE is presently at IRSID, 34 rue de la Croix de Fer, F-78105 Saint-Germain-en-Laye cedex, France

Materials and apparatus

Materials

Three materials (table I) with various surface roughnesses (table II) :
- AISI 1045 steel (0.46 wt % C) in the annealed state,
- Pure cast nickel,
- Conventinally heat treated Inconel 718.

Table I : Chemical composition (weight percent).

	Fe	Ni	Cr	Nb	C	Mn	Si	S	P	Al	Mo	Ti	Co
Steel 1045	Bal.	-	-	-	0.466	0.33	0.19	0.01	0.01	-	-	-	-
Nickel	0.02	99.9	-	-	0.003	-	0.001	0.001	0.001	-	-	-	-
Inco. 718	18.1	Bal.	18.0	5.15	0.03	0.08	0.12	0.01	0.01	0.41	2.95	0.94	0.47

Table II : Surface roughnesses
(R_a : arithmetic average roughness, R_z : peak-to-peak roughness depth and R_m the maximal depth).

		R_a (µm)	R_z (µm)	R_m (µm)
Steel 1045	ground	0.36 ± 0.06	2.25 ± 0.5	2.6 ± 0.5
	sandblasted	0.95 ± 0.04	7.80 ± 0.7	9.4 ± 0.9
	polished	0.02 ± 0.03	0.30 ± 0.08	0.3 ± 0.1
Nickel	ground	0.53 ± 0.08	3.60 ± 0.7	4.2 ± 0.8
	polished	0.01 ± 0.01	0.2 ± 0.1	0.3 ± 0.1
Inconel 718	ground	0.37 ± 0.05	2.65 ± 0.3	3.6 ± 0.4
	milled	2.80 ± 0.22	10.1 ± 2.2	10.5 ± 3.0
	polished	0.01 ± 0.01	0.15 ± 0.1	0.2 ± 0.1

For handling, steel is immersed in glycerine to prevent oxidation, which is not required for nickel and Inconel 718. All surfaces are carefuly cleaned before being irradiated.

Experimental

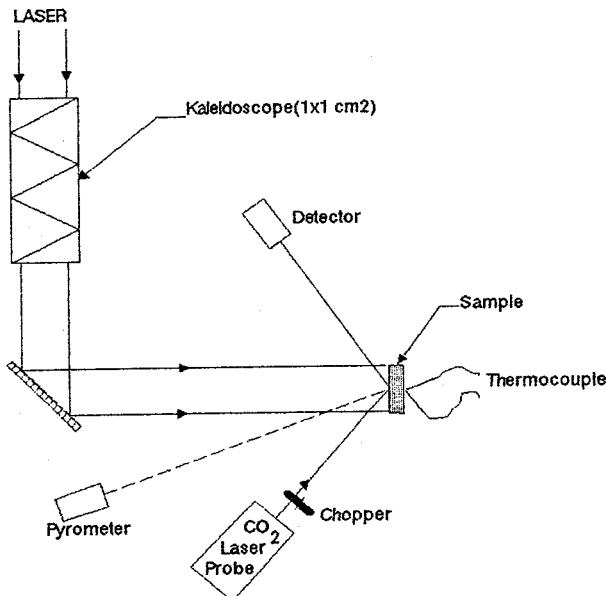### *Thermal method at 10.6 µm (CO_2)*

LASER

Kaleidoscope(1x1 cm2)

Detector

Sample

Thermocouple

Pyrometer

CO_2 Laser Probe

Chopper

The source is a 5 kW Spectra-Physics cw-CO_2 laser with an unpolarized and multiple mode beam. An homogeneized top-hat beam is obtained using a kaleidoscope (figure 1). The parallelipedic sample (10 x 10 x 1 mm³) is put onto three tungstene pits, which minimize thermal losses. The absence of gas shielding for all experiments induces oxidation. The laser beam irradiates the whole square surface of the sample with a mean power density ranging from 5.10^6 W/m² to 9.10^6 W/m². Temperature is monitored by a chromel-alumel thermocouple welded to the sample bottom.

Since A_i is used to calculate $T_c(t_i,e)$, iterations are required to obtain the best result. Consequently, absorption results are obtained from iterative solving of the one-dimensional thermal problem using finite element calculations [3] which consist in minimizes the following functional :

Figure 1 : Experimental setup used at 10.6 µm.

$$J(A_1,...,A_N) = \frac{1}{2}\sum_{i=1}^{N}[T_m(t_i,e) - T_c(t_i,e)]^2 \tag{1}$$

with A_i absorptivity for $[t_{i-1}, t_i]$, e sample thickness, T_m and T_c measured and calculated temperatures.

In these calculations, variable thermal properties (i. e. thermal conductivty and specific heat) of the material are involved although these values are equilibrium one, which reduces the accuracy. Absorptivity results could be given as a function of temperature or time.

Reflectivity measurements at 1.06 μm (Nd-YAG)

A 250 W mean output power "Lasag" Nd-YAG laser with an unpolarized beam was used. The previously-described thermal method cannot be used because of the low power and low repetition rate. Reflectivity measurements are therefore carried out with a sphere (figure 2) which integrates the reflected part of the beam. A single Nd-YAG laser pulse is focused on the sample. The pulse duration is 15 ms and the incident mean power density of about 5.10^8 W/m^2.
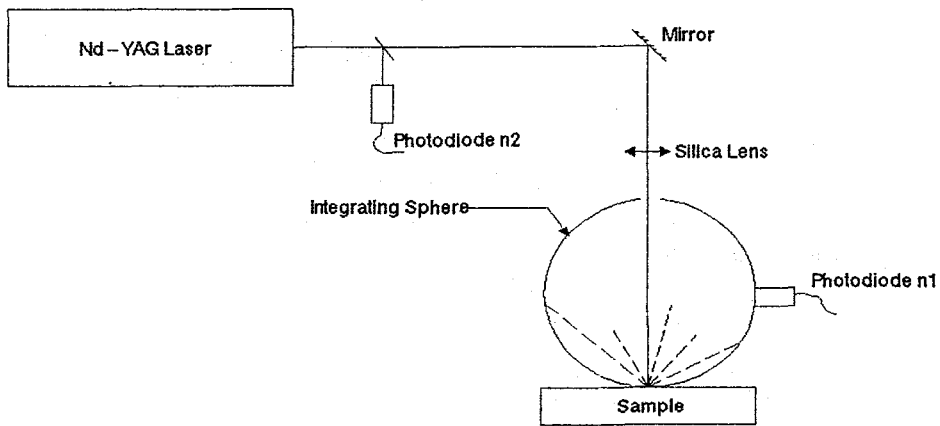

Figure 2 : Experimental arrangement for the reflectance measurements at 1.06 μm.

The photodiode number 1 signal (reflected intensity) over the signal number 2 (incident intensity) gives, after previous calibration with a gilded molybdenum mirror, the reflectivity. Then, the absorptivity results from substracting the reflectivity to 1 because the tested materials are not transparent. However, the as measured absorptivity can only be given as a function of pulse duration since temperature is heterogeneous at the irradiated surface. Temperature increase has been calculated at the center and at the periphery of the impact using finite elements. This can be applied because the power density is known, the spatial intensity is multimode (as monitored with a CCD camera), the intensity versus time is recorded and finally the absorptivity is measured as a function of time. Figure 3 shows the results for sand blasted steel and give some indications about temperatures attained during these experiments which will be used in a further discussion.

Consequently, absorptivity could be estimated as a function of temperature ; first, by eliminating the time dependence between the experimental result A(t) and calculated T(t) ; second, by extrapolating this new dependence A(T) to the whole time range (outside [0,15 ms]). This will be used in the discussion.
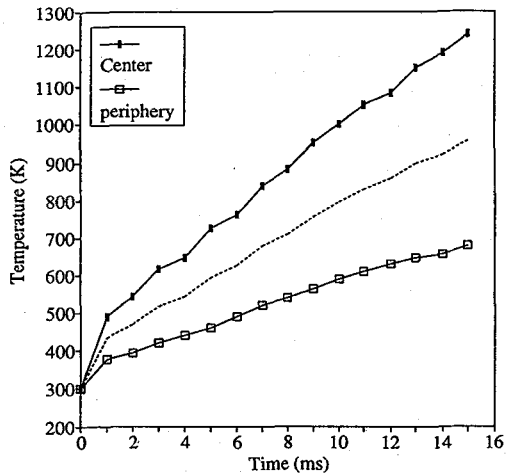
Figure 3 : Calculated temperatures at center and periphery of the impact for sandblasted steel.

Results [5]

AISI 1045 steel

Figure 4 shows the absorptivity measured at 10.6 μm as a function of temperature and at 1.06 μm as a function of pulse duration for a given power density noted π and mesured in W/m^2. The scatterband bars for 10.6 μm measurements are obtained from the envelope of all curves corresponding to three or five experiments in the same conditions. At 1.06 μm, the reproducibility always ranges in ± 0.03.

a) at 10.6 μm (CO_2)   b) at 1.06 μm (Nd-YAG)

$\pi = 5.10^6$ W/m², 400 < (dT/dt)$_{max}$ < 475 K/s $\pi = 2.10^8$ W/m², (dT/dt)$_{max}$ ≈ 6.10⁴ K/s
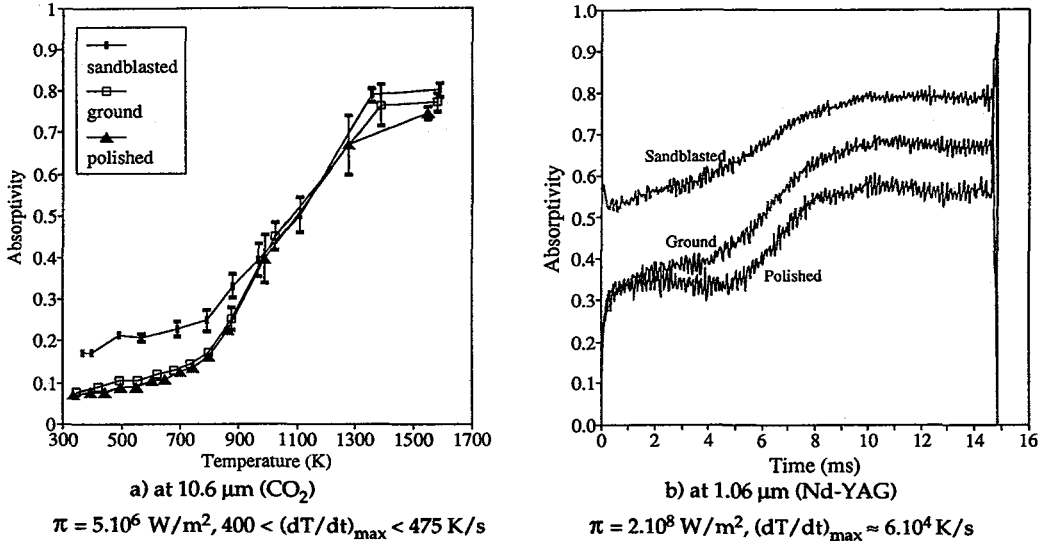
<u>Figure 4</u> : Absorptivity measurements for steel.

At room temperature, absorptivity is lower at 10.6 μm (0.08 to 0.20) than at 1.06 μm (0.30 to 0.52). Moreover, in both cases it greatly depends on surface roughness. It also increases with temperature due to surface oxidation. Roughness plays no part at 10.6 μm when temperature increases, contrary to what observed at 1.06 μm. This is probably due to the surface oxidation kinetics and optical differences between the two wavelengths.

Nickel

a) at 10.6 μm (CO_2)   b) at 1.06 μm (Nd-YAG) for polished surface

$\pi = 5.10^6$ W/m², 100 < (dT/dt)$_{max}$ < 130 K/s $\pi = 3.10^8$ W/m², (dT/dt)$_{max}$ ≈ 130 K/s
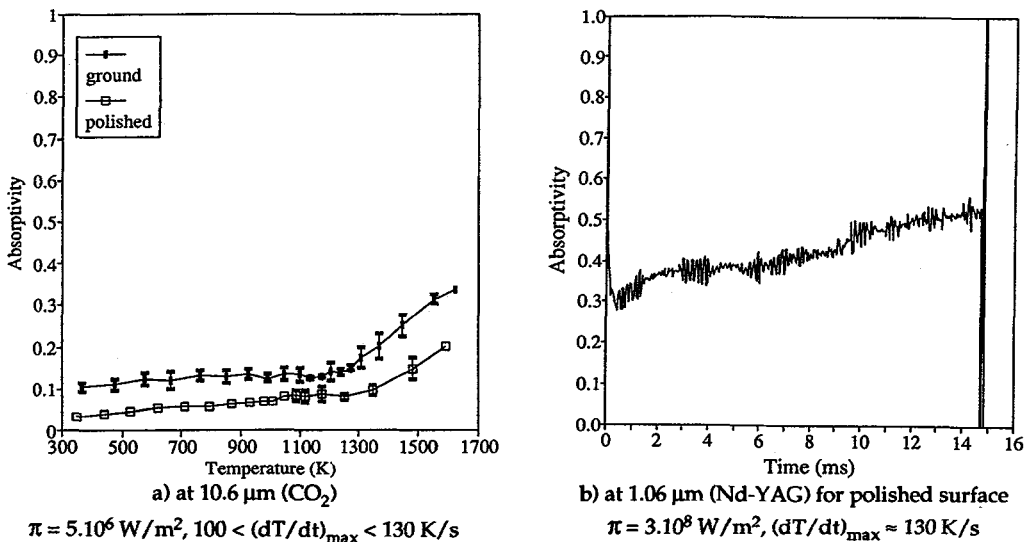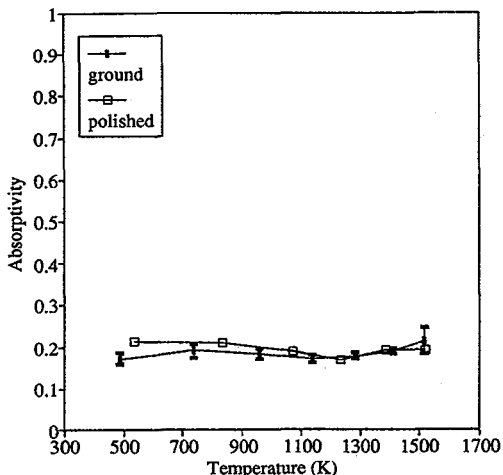
<u>Figure 5</u> : Absorptivity measurements for nickel.

Absorptivity measurements at 10.6 µm as a function of temperature and at 1.06 µm as a function of pulse duration are exhibited in figure 5. At room temperature, absorptivity is lower for 10.6 µm (0.04 to 0.10) than for 1.06 µm (0.30). When temperature increases, absorptivity does not vary very much for the two wavelengths, the surface oxide is probably transparent or very thin, which prevents any influence on the result.
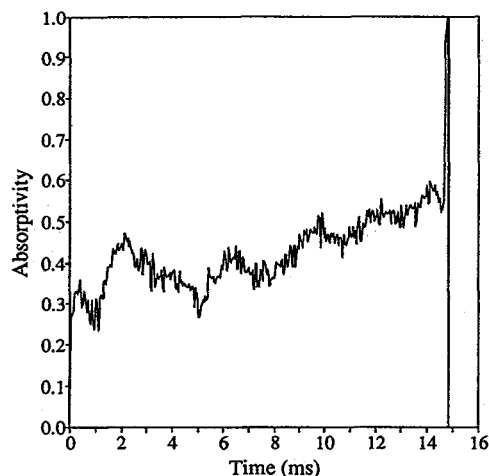
Inconel 718

Figure 6 shows the absorptivity results for Inconel 718. At 10.6 µm. Whatever the temperature, absorptivity remains almost the same, i.e. about 0.25 as mesured at a high temperature (1500 K). For 1.06 µm, absorptivity is higher (0.30) and increases with temperature up to 0.55. The oscillations, systematically occured and are reproducible which is probably due to interference phenomenons in the developing oxide.

a) at 10.6 µm (CO_2)

$\pi = 9.10^6$ W/m^2 and $(dT/dt)_{max} \approx 250$ K/s

b) at 1.06 µm (Nd-YAG) for polished surface

$\pi = 7.10^8$ W/m^2 and $(dT/dt)_{max} \approx 6.10^4$ K/s

Figure 6 : Absorptivity measurements for Inconel 718.

Discussion

Absorptivity

The differences between the methods used for the two wavelengths prevents easy direct comparison. Hoever, a significant comparison can be done using the extreme values, i.e. initial (at room temperature) and final (at elevated temperature) absorptivities (table III). One must also keep in mind that the duration of the irradiations, power density, thermal cycle and oxidation rate are very different for the two wavelengths.

Table III : Absorptivity comparison at 10.6 and 1.06 µm.

		CO$_2$ (10.6 µm)					Nd-YAG (1.06 µm)				
		Absorptivity (%)		Temperature (K)			Absorptivity (%)		Temperature (K)		
		initial	final	initial	final	$\Delta A/A_i$	initial	final	initial	final	$\Delta A/A_i$
Steel	sand	17	80	400	1600	371	52	78	300	1240	50
	grou.	8	80	350	1500	900	32	67	300	1090	109
	polish.	7	75	350	1500	971	31	57	300	1100	84
Nickel	polish.	4	20	350	1550	400	32	52	300	980	62
Inco.	polish.	22	20	500	1500	- 9	30	55	300	1180	83

$\Delta A / A_i$ is expressed as follows :

$$\frac{\Delta A}{A_i}(\%) = \frac{A_{final} - A_{initial}}{A_{initial}} \times 100 \qquad (2)$$

This ratio features the increase of absorptivity, which therfore gives an idea of the heat flow variation during irradiation. In the second part of the discussion, an illustration of the so called "thermal runaway" will be given for thermal cycles calculated using the previous absorptivity results.

For all surfaces (table III), absorptivity at room temperature is higher for the 1.06 µm light than for the 10.6 µm light. The difference seems to be promoted by a roughness decrease. Among the studied metals, Inconel 718 shows the smallest absorptivity increase when irradiating at 1.06 µm. Regarding this property, the material order is then : nickel and steel.

As already mentioned, the absorptivity increase, quantified by $\Delta A / A_i$, can be used to feature the influence on thermal runaway. Roughness is generally a limiting factor, mainly due to a higher initial absorptivity as experimentaly ascertained. $\Delta A / A_i$ is much higher at 10.6 µm (CO_2) than at 1.06 µm (Nd-YAG) except for Inconel 718. It has to be related with the initial absorptivity because the maximum of $\Delta A / \Delta T$ is approximately the same for 1.06 and 10.6 µm (0.10 %/K).

Thermal cycles

Absorptivity measurements are then used to calculate thermal cycles for various heat flow inputs. Finite element calculations ("Zébulon" code) involve thermal properties as a function of temperature (thermal conductivity and specific heat) and a variable heat flow (i. e. the initial power density multiplied by the measured absorptivity). The motion of the laser beam is not taken in account. Figures 7-a and 7-b give respectively the thermal cycle at 10.6 and 1.06 µm for the sand blasted steel with a pulse duration of one second. Thermal cycles for 1.06 µm are calculated as mentioned earlier.

a) at 10.6 µm (CO_2)   b) at 1.06 µm (Nd-YAG)

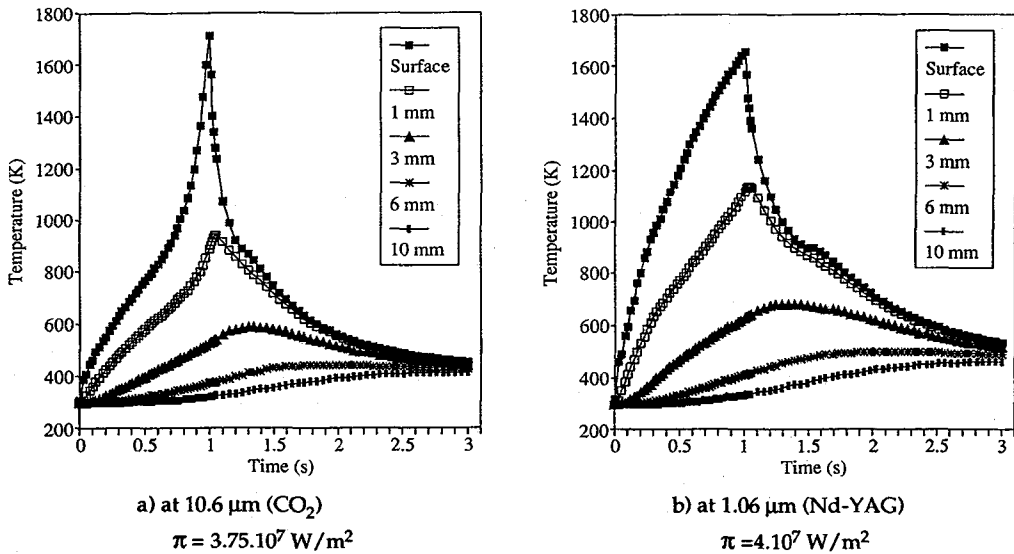$\pi = 3.75.10^7 \text{ W/m}^2$ $\pi = 4.10^7 \text{ W/m}^2$

Figure 7 : Thermal cycles for different deeps calculated with variable absorptivity versus temperature.

Thermal runaway (i. e. the heating rate suddenly increases) clearly appears above 900 K for 10.6 µm, it is due to surface oxidation which induces a higher absorptivity level. For 1.06 µm, this phenomenon does not occur, which suggests that surface treatment of steel without any coating (e. g. graphite) is easy to control, this has been experimentally ascertained. The shape of the thermal cycles obtained at 1.06 µm (figure 7-b) is also appropriate from a metallurgical point of view because the holding time at an elevated temperature is higher than at 10.6 µm. Cooling at the surface clearly shows a recalescence phenomenon which is not real but only due to the fact that the calculations used do not involve the martensitic transformation.

Conclusion

Absorptivities at two wavelengths 10.6 μm (CO_2) and 1.06 μm (Nd-YAG) for three materials (i. e. AISI 1045 steel, nickel and Inconel 718) were determined between room temperature and more than 1000 K in fairly realistic dynamic conditions. All experiments have been carried out in air without any gas shielding. Oxide layer formation increases the energy absorbed by the metal in particular for steel at 10.6 μm. This induce a sudden growth of temperature, i.e. the so called "thermal runaway", and gives experimental difficulties to control the treatment. For surface hardening of steel with CO_2 laser, this phenomenon can be generally prevented by previous graphite spraying before processing.

Typical thermal cycles calculated for steel at the two laser wavelengths clearly show a difference regarding the thermal runaway. The Nd-YAG wavelength allows treatment without any coating or gas shielding, which prevents pollution and improves the reliability of the process compared to CO_2 treatments. This has been experimentally ascertained. In spite of this advantage and of the beam handling, Nd-YAG lasers generally operate in the pulsed mode which is not suitable for surface treatments.

This study clearly shows the prominent role of adequate measuring of absorptivity. A standard method remains to be defined. A combination of the thermal and optical methods used can be suggested.

References

[1] WIETING T.J. and DE ROSA J.L., "Effects of surface condition on the infrared absorptivity of 304 stainless steel", J. Appl. Phys., vol. 50, 2, (1979), 1071.

[2] STERN G., "Absorptivity of cw CO_2, CO and Nd-YAG laser beams by different metallic alloys", Proc. of the 3rd European Conference on Laser Treatment of Materials, ECLAT'90, Sept. 17-19, 1990, Erlangen, Germany, Ed. by BERGMANN H.W. and KUPFER R., Pub. by Sprechsaal Publishing Group, Corburg, Germany, (1990), 25.

[3] KECHEMAIR D., "Contribution à l'étude de l'interaction laser-matière : Instrumentation et optimisation de la trempe superficielle des aciers par laser CO_2 continu", Ph. D. Thesis, Spécialité Optique et Photonique, Paris XI, (1989).

[4] PATEL R.S. and BREWSTER M.Q., "Effect of oxidation on low power Nd-YAG laser metal interaction", ICALEO'88, Oct. 30 - Nov. 4, (1988), Santa-Clara, CA, USA, Pub. by Springer Verlag / IFS, 1989, 313.

[5] SAINTE-CATHERINE C., "Etude des possibilités d'applications des lasers Nd-YAG de forte puissance aux traitements de surfaces", Ph. D. Thesis, Spécialité Sciences et Génie des Matériaux, Ecole des Mines de Paris, Dec. (1990).